



Published in final edited form as:

Ann Otol Rhinol Laryngol. 2008 May ; 117(5): 327–334.

Optical Coherence Tomography of the Newborn Airway

James M. Ridgway, MD, Jianping Su, MS, Ryan Wright, Shuguang Guo, PhD, David C. Kim, MD, Roberto Barretto, MD, Gurpreet Ahuja, MD, Ali Sepehr, MD, Jorge Perez, Jack H. Sills, MD, Zhongping Chen, PhD, and Brian J. F. Wong, MD, PhD

From the Department of Otolaryngology–Head and Neck Surgery (Ridgway, Barretto, Ahuja, Sepehr, Wong), the Beckman Laser Institute (Ridgway, Su, Wright, Guo, Sepehr, Perez, Chen, Wong), the Department of Biomedical Engineering (Su, Guo, Chen, Wong), and the Department of Pediatrics (Kim, Sills), University of California–Irvine, Irvine, California.

Abstract

Objectives—Acquired subglottic stenosis in a newborn is often associated with prolonged endotracheal intubation. This condition is generally diagnosed during operative endoscopy after airway injury has occurred. Unfortunately, endoscopy is unable to characterize the submucosal changes observed in such airway injuries. Other modalities, such as magnetic resonance imaging, computed tomography, and ultrasound, do not possess the necessary level of resolution to differentiate scar, neocartilage, and edema. Optical coherence tomography (OCT) is an imaging modality that produces high-resolution, cross-sectional images of living tissue (8 to 20 μm). We examined the ability of this noninvasive technique to characterize the newborn airway in a prospective clinical trial.

Methods—Twelve newborn patients who required ventilatory support underwent OCT airway imaging. Comparative analysis of intubated and non-intubated states was performed.

Results—Imaging of the supraglottis, glottis, subglottis, and trachea was performed in 12 patients, revealing unique tissue characteristics as related to turbidity, signal backscattering, and architecture. Multiple structures were identified, including the vocal folds, cricoid cartilage, tracheal rings, ducts, glands, and vessels.

Conclusions—Optical coherence tomography clearly identifies *in vivo* tissue layers and regional architecture while offering detailed information concerning tissue microstructures. The diagnostic potential of this technology makes OCT a promising modality in the study and surveillance of the neonatal airway.

Keywords

imaging; newborn airway; optical coherence tomography; subglottic stenosis

© 2008 Annals Publishing Company. All rights reserved.

Correspondence: Brian J. F. Wong, MD, PhD, or Zhongping Chen, PhD, Beckman Laser Institute, University of California–Irvine, 1002 Health Sciences Rd, Irvine, CA 92612; bjwong@uci.edu or z2chen@uci.edu.

Presented as a podium discussion at the meeting of the American Broncho-Esophagological Association, San Diego, California, April 26–27, 2007. Recipient of the Seymour R. Cohen Award.

Copyright of *Annals of Otolaryngology & Laryngology* is the property of Annals Publishing Company and its content may not be copied or emailed to multiple sites or posted to a listserv without the copyright holder's express written permission. However, users may print, download, or email articles for individual use.

INTRODUCTION

Laryngeal stenosis of the newborn is described as a narrowing of the supraglottic, glottic, or subglottic regions. The most common site of this airway narrowing is at the level of the subglottis. In a newborn patient, this condition may pass undetected or present as a life-threatening and, at worst, a life-ending event. The ability to diagnose, treat, and even prevent subglottic stenosis has been the hallmark of medical advances in neonatal care, as well as the harbinger of continued controversy and debate.

The architecture of the newborn subglottis is unique, as the cricoid cartilage is the only circumferential ring of the upper airway. This anatomic configuration makes the narrowest point of the newborn airway also its most uncompromising.^{1,2} Further, the tissues of the subglottis are delicate in nature, are easily damaged, and rapidly develop edematous changes. These circumstances, when taken together, significantly predispose the subglottis to inflammation, scar formation, and stenosis in newborn patients who require endotracheal intubation.

Direct laryngoscopy and bronchoscopy has remained the gold standard in the evaluation of newborns in whom subglottic stenosis is suspected.³ Unfortunately, this technique is limited to the characterization of the surface anatomy and does not offer detailed analysis of the subepithelial tissues. During direct laryngoscopy and bronchoscopy, airway trauma may be incurred with the removal of the endotracheal tube, the use of surgical endoscopes, or the (re) placement of a breathing tube if respiratory distress or airway disease is observed. This clinical circumstance is often complicated, as the pulmonary, cardiac, and hypoxic thresholds in the newborn population may postpone the evaluation of the airway because of limited tolerances to physiologic stress. In essence, the ultimate challenge in the evaluation of the newborn airway is to minimize diagnostic trauma and physiologic stress while accurately characterizing the laryngeal tissues.

Optical coherence tomography (OCT) is an imaging modality that utilizes non-ionizing coherent light to produce high-resolution images of living tissues.⁴ The images are produced in a cross-section format, similar to that of ultrasonography, but with a resolution of 10 μm and a depth of nearly 2 mm. This high-resolution modality allows one to distinguish the epithelium from the underlying tissue microstructures on the basis of optical scattering, absorption, and anisotropy with near-real-time frame rates. Using OCT imaging, one can noninvasively characterize living tissues beyond the current imaging capacities of magnetic resonance imaging, computed tomography, and ultrasound.^{5,6}

The current investigation reviews OCT imaging of the newborn airway and its potential role in the management of intubated newborn patients. The aims of this study were to apply OCT technology in the characterization of tissue architecture, review imaging in intubated and non-intubated states, and define the feasibility of this modality in this given population. Briefly, we will discuss OCT image acquisition, interpretation, and operative instrumentation, followed by a review of our series of newborn patients. To the best of our knowledge, this is the first report of OCT imaging of the newborn airway.

METHODS

Patient Population and Endoscopy

Optical coherence tomography imaging was performed on 12 patients at the University of California–Irvine Medical Center under a protocol approved by the Human Subjects Institutional Review Board at the University of California–Irvine. The study subjects were limited to newborn patients who required endotracheal intubation with mechanical respiratory

support. While the patients were under general anesthesia in the operating room or light sedation in the newborn intensive care unit, OCT Imaging was performed with the use of a custom handheld probe. Multiple sites of the airway tract were imaged. Endoscopic photographs were only obtained in patients who were undergoing surgical endoscopy.

OCT System and Instrumentation

The OCT system and instrumentation has been previously described and will be briefly reviewed.^{7,8} Near-infrared light from a broadband light source (central wavelength $\lambda = 1,310$ nm; full width at half maximum $\Delta\lambda = 80$ nm; BBS 1310, AFC Technologies Inc, Hull, Canada) enters a 2×2 fiberoptic coupler. In the reference arm, a rapid scanning optical delay line attains A-scan at 500 Hz without phase modulation. The phase modulator generates 500-kHz phase modulation for heterodyne detection. Signals backscattered from the sample arm are obtained by phase-resolved processing with the interference fringes. The axial resolution of the system in tissue is approximately $7 \mu\text{m}$, and the lateral resolution approaches $20 \mu\text{m}$. The horizontal image window is set laterally from 2 to 6 mm in length, and detailed images of tissue microstructure are recorded up to a depth of 1.6 mm, depending upon the turbidity of the media.

For imaging the newborn airway in vivo, a custom flexible probe and a rigid OCT probe were designed to accommodate the specific anatomic considerations during endoscopy and the curvature of the endotracheal tube. The probes consist of a $900\text{-}\mu\text{m}$ single-mode fiber distally terminated by a gradient refractive index (GRIN) lens and a 0.5-mm right angle prism (Fig 1). The GRIN lens is 0.7 mm in diameter and works to focus light. Mounting of the prism and GRIN lens is accomplished with an optics-grade, low-viscosity, wicking ultraviolet glue. Scanning is achieved by linearly translating the optical fiber along the long axis by means of a motorized piezo-driven stage (model 663.4pr, PI Line, Tustin, California). The optical fiber, the optical elements, and a supportive stainless steel tube are enclosed within a transparent plastic tube ($2,000\text{-}\mu\text{m}$ outer diameter, $200\text{-}\mu\text{m}$ thickness, fluorinated ethylenepropylene material). Two different models of the steel tube were utilized for this project. One stainless tube was entirely rigid for use during surgical endoscopy, and a flexible vertebrated steel tube was used for imaging across the endotracheal tube (Fig 2). For orienting the user, colored markings were made along the sides of the optical fiber with light exiting along the opposite side of the fiber tip. This system design remained constant for all subjects studied.

OCT Imaging

Images were obtained either at the time of surgical endoscopy, by placing the probe through a laryngoscope with the patient in laryngeal suspension, or in the neonatal intensive care unit, by placing the imaging probe through a circuit adaptor into the endotracheal tube. Image production was directed by the orientation of light propagation as it exited the tip of the OCT fiber and was confirmed before imaging with the use of a reference infrared sensor card (Newport Corp, Irvine, California). During surgical endoscopy, the tip of the OCT probe was placed in near-contact to the region of interest with the image visualized on a bedside satellite cart monitor. Trans-endotracheal imaging was performed with direct approximation of the flexible OCT probe to the inner surface of the endotracheal tube with image visualization made from an OCT monitor tower. The OCT imaging was systematically performed throughout the airway along the anterior, right lateral, posterior, and left lateral positions with the probe drawn from the distal to the proximal airway. The OCT video files were subsequently transferred to a database in which still digital images were captured and catalogued. The image orientation remained constant, with left and right sides of the images representing the proximal and distal regions of the newborn airway. The superior and inferior aspects of the image, respectively, illustrate the surface mucosa and the inner microstructures of the regions of interest.

OCT Image Analysis

Images from multiple sites along the aerodigestive tract were obtained. The images were then sorted into 4 anatomic groups: 1) trachea, 2) subglottis, 3) glottis, and 4) supraglottis. Further comparisons were made between direct imaging of the newborn airway and images obtained by OCT imaging through the endotracheal tube. A review of basic newborn parameters at the time of OCT imaging is presented in the Table.

RESULTS

Twelve newborn subjects ranging from 24 to 41 weeks of gestational age participated in an OCT study of the airway with emphasis on intubated and non-intubated states. Cross-sectional images were collected from multiple sites during OCT imaging. All patients underwent imaging of the supraglottic, glottic, subglottic and tracheal regions. Imaging was performed in 4 quadrants that were equally spaced and aligned with anterior, posterior, right lateral, and left lateral positions. Database images were reviewed, categorized, and partitioned on the basis of anatomic structures. Attention was also given to images that demonstrated characteristics not commonly observed in other subjects or at other sites.

The following images represent an analysis of tissues in which epithelium, basement membrane, lamina propria, and other regional microstructures were clearly identified in normal tissues by OCT (group 1). Each OCT image represents a specific region of interest, as well as intubated and non-intubated states. Figure 3 displays a classic OCT image of the trachea with clear delineation between the epithelium and the underlying lamina propria along the basement membrane interface. Differences in grayscale intensity are directly related to the degree of the optical signal that is backscattered (reflected) by a given medium. Tissues with a relatively high turbidity create greater backscatter signals (eg, cartilage) and are represented in a grayscale distribution as a color closer to white. Tissues with a low optical scattering coefficient are represented by a darker appearance (eg, water). Such differences allow the viewer to discern an image on the basis of the variable optical densities of a given tissue. As seen in Fig 3, the optical density of the epithelium is less than that of the lamina propria or underlying tracheal cartilage. In Fig 4, we see a minor decrease in overall signal intensity, but we are readily able to discern the epithelium, lamina propria, and tracheal cartilages. This image was produced by trans-endotracheal OCT imaging in which the OCT fiber was inserted into the endotracheal tube and the optical signal was transmitted through the tube and into the surrounding tissues. One may note the difference in the size of the tracheal cartilages between Figs 3 and 4. These findings represent the 15-week developmental difference between these two patients.

In group 2, the cricoid cartilage is well delineated against the overlying tissues and glands (Fig 5). The loss of signal beyond the cricoid cartilage denotes its optical density in comparison to the surrounding tissues. The heterogeneity of the optical signal within the lamina propria represents the distribution of seromucinous glands (darker regions). On the right side of the image is a hysteresis artifact from the OCT translational stage. The boundaries of the remaining subglottis are observed in Fig 6. Along the left side of the image, the homogeneous signal of the vocal fold is a considerable contrast to the more complex signal of the distal subglottis observed on the right. In the intubated newborn (Fig 7), the subglottis is once again imaged through the substance of the endotracheal tube. Little information is lost, as the epithelium, lamina propria, glandular, and cricoid boundaries are well visualized.

Tissues devoid of microstructural features, such as glands or ducts, are relatively homogeneous in OCT imaging and can represent the vocal fold, granulation tissue, or even scar. The last two are often devoid of the normal interface of the epithelium and underlying lamina propria. This is best represented by Fig 8 from group 3, in which OCT imaging of a normal vocal fold is resolved. As imaging is performed in the more proximal airway (group 4), one can see the

apposition of the glandular false vocal fold and the vocal fold with the partition of the collapsed ventricle in between (Fig 9).

Figure 10 represents the patient in this study who was intubated for a period of 61 days at the time of OCT imaging. In this image of the subglottis, one can appreciate the two sites of clustered dark regions. As described in previous publications,^{9,10} fluids with similar density to that of water allow for greater signal propagation into tissues due to limited backscattering. The result is greater signal penetration and ultimately greater image clarity at depths that would not otherwise be observed in a more turbid medium. In contrast, blood absorbs the OCT signal and creates a shadow effect in which underlying structures are poorly observed. Taken together, these regions likely represent occluded glandular ducts, inflammatory changes, or recent trauma. There is also similar optical density of the epithelium and lamina propria in these regions as well.

In the circumstance of poor image quality altogether, one must consider the possibility that other components in the newborn airway may absorb or backscatter the OCT signal. The image in Fig 11 represents a fluid that was lining the outside of the endotracheal tube that nearly absorbed the entire optical signal. On further evaluation of the patient's history, the infant was noted to have frank reflux observed in the morning and was started on antireflux therapy before OCT imaging.

DISCUSSION

Narrowing of the subglottic airway can represent a congenital, acquired, or combined process. Congenital stenosis implies that the narrowing of the laryngeal apparatus is a preexisting condition not created by acts of medical intervention or therapy. Often this form of narrowing is associated with other malformations or syndromes involving the head and neck. However, congenital narrowing of the airway may predispose a newborn to the development of subglottic stenosis if airway instrumentation or intubation is required. In the circumstance of acquired subglottic stenosis, laryngeal injury is often related to intubation and/or other medical interventions that can lead to soft tissue trauma and inflammation. This form of stenosis is suspected to represent the majority (95%) of clinical cases observed and has defined our focus of investigation.^{11,12}

In this study we present our experience with 12 newborn patients who underwent OCT imaging of the airway. With each patient studied, OCT imaging was able to resolve surface epithelium, the underlying lamina propria, and the interface of the basement membrane in all tissues of the laryngeal airway. In the majority of patients imaged, we were able to visualize the interface of the supraglottic, glottic, subglottic, and tracheal regions. The characterization of the newborn airway is of exceptional value in the neonatal setting, as operative endoscopy does not possess the ability to view into tissues and magnetic resonance imaging, computed tomography, and ultrasonography do not possess the spatial resolution necessary to evaluate processes at the microscopic level. Additionally, operative endoscopy may need to be delayed in those patients whose conditions are too unstable and pose too much of an operative risk for them to be brought from the neonatal intensive care unit to the operating room for evaluation. The ability to noninvasively image the newborn airway with a high-resolution imaging modality would significantly aid the pediatric otolaryngologist and perinatologist in the care of a newborn who requires long-term intubation.

Optical coherence tomography is a noninvasive technology that does not 1) produce ionizing radiation, 2) require patient extubation, 3) add physiologic stress in a mechanically ventilated patient, or 4) significantly contribute to the risk of subglottic stenosis. In this current application, OCT was conducted with near-real-time image and video production with

associated live-feed audio. This technology has been well established in multiple fields of laboratory and medicine research and provides the ability to microscopically view tissues without the limitations, complications, and artifacts inherent in current operative techniques. It is important to reiterate that all trans-endotracheal imaging performed in this study was conducted from within the confines of the endotracheal tube. The imaging fiber, with its associated housing, did not exceed 2 mm in diameter. As a comparison, the diameter of the OCT probe is less than that of the standard newborn endotracheal suction catheter used in daily maintenance and hygiene of the intubated airway.

Currently, multiple clinical investigations are under way in which OCT imaging technology is being applied to characterize various tissue and disease states. In the field of ophthalmology, OCT imaging has become an invaluable tool with current clinical applications in the imaging of macular edema, choroidal neovascularization, and glaucomatous changes. Other medical fields currently investigating OCT imaging include cardiology, gastroenterology, hepatology, pulmonology, and urology.^{6,13–16} Investigative studies of OCT technology in the field of otolaryngology have also led to various potential applications of this imaging modality.^{5,9,10,17–20}

This study represents the first efforts to characterize the newborn airway by use of OCT imaging technology. Correlation of OCT images in intubated and non-intubated patients revealed only minor reduction in the optical signal while continuing to resolve the various tissue layers and microstructures of the laryngotracheal apparatus. Studies of various intubation timelines further revealed tissue changes that may not be otherwise appreciated or revealed with current techniques that require the removal of the endotracheal tube.

There are a number of limitations and challenges in the study presented. Of the 12 patients imaged, only 1 patient was free of prior intubation trauma or airway assistance. The limited number of patients in this study also prevented us from drawing any diagnostic conclusions beyond the imaging capabilities of OCT technology. However, such difficulties are inherent in a pilot study and create a mandate for further investigation and discussion of this topic. We have also discovered a number of challenges when applying this technology, each of which can compromise image quality. There is a learning curve, as with many operative techniques, in which an individual and a team are to become accustomed to a technique or procedure. The surgeon must coordinate the positioning of the OCT probe on the basis of known anatomy and image reference, much like the cardiologist who performs ultrasound in the evaluation of the heart. It is important to note that the probe position must be adjusted to create the optimal image for future analysis and that such actions require a working knowledge of image interpretation.

Although the incidence of subglottic stenosis has declined considerably over the past three decades, the ability to perform *in vivo* tissue imaging with a noninvasive, high-resolution modality could significantly alter the management of the newborn airway. With the capability to perform studies at or near video rates, one could easily complete initial and weekly evaluations of high-risk newborns who require long-term ventilator assistance. Of important note is the relatively recent application of this modality in the head and neck with rapid improvements in image resolution, speed of image production, and evolution of clinical instrumentation.

Optical coherence tomography is a novel imaging modality that allows for noninvasive imaging of the newborn airway in intubated and non-intubated states. With its high-resolution capabilities, OCT is able to resolve the tissues of the intubated newborn airway without creating physiologic stress or inducing soft tissue injury. These findings, although preliminary, have reaffirmed our clinical investigation of this promising modality. To this end, we will continue

to develop our experience in the newborn population, as well as advance our understanding of the potential clinical applications of OCT.

Acknowledgments

The authors thank master machinists Rudolph Limburg and Steve Knisley for assistance with construction of the instrumentation. We thank the nurses and respiratory therapist of the UC Irvine Neonatal Intensive Care Unit for their efforts, as well as Aya Yamamoto, RN, for her help and patience in the operating room. The US Government is authorized to reproduce and distribute reprints for Governmental purposes notwithstanding any copyright notation. The views and conclusions contained herein are those of the authors and should not be interpreted as necessarily representing the official policies or endorsements, either expressed or implied, of the Air Force Research Laboratory or the US Government.

This work was supported by the National Institutes of Health (DC 006026, CA 91717, EB 00293, RR 01192, M01-RR00827-28), the Flight Attendant Medical Research Institute (32456), the State of California Tobacco Related Disease Research Program (12RT-0113), the Air Force Office of Scientific Research (FA9550-04-1-0101), and the Arnold and Mabel Beckman Foundation.

REFERENCES

1. Sherman JM, Lowitt S, Stephenson C, Ironson G. Factors influencing acquired subglottic stenosis in infants. *J Pediatr* 1986;109:322–327. [PubMed: 3734970]
2. Holinger PH, Kutnick SL, Schild JA, Holinger LD. Subglottic stenosis in infants and children. *Ann Otol Rhinol Laryngol* 1976;85:591–599. [PubMed: 791051]
3. Holinger LD. Diagnostic endoscopy of the pediatric airway. *Laryngoscope* 1989;99:346–348. [PubMed: 2918809]
4. Huang D, Swanson EA, Lin CP, et al. Optical coherence tomography. *Science* 1991;254:1178–1181. [PubMed: 1957169]
5. Wong BJ, Jackson RP, Guo S, et al. In vivo optical coherence tomography of the human larynx: normative and benign pathology in 82 patients. *Laryngoscope* 2005;115:1904–1911. [Erratum in *Laryngoscope* 2006;116:507.]. [PubMed: 16319597]
6. Gerckens U, Buellfeld L, McNamara E, Grube E. Optical coherence tomography (OCT). Potential of a new high-resolution intracoronary imaging technique. *Herz* 2003;28:496–500. [PubMed: 14569390]
7. Zhao Y, Chen Z, Saxer C, et al. Phase-resolved optical coherence tomography and optical Doppler tomography for imaging blood flow in human skin with fast scanning speed and high velocity sensitivity. *Optics Lett* 2000;25:114–116.
8. Ren H, Ding Z, Zhao Y, et al. Phase-resolved functional optical coherence tomography: simultaneous imaging of in situ tissue structure, blood flow velocity, standard deviation, birefringence, and Stokes vectors in human skin. *Optics Lett* 2002;27:1702–1704.
9. Armstrong WB, Ridgway JM, Vokes DE, et al. Optical coherence tomography of laryngeal cancer. *Laryngoscope* 2006;116:1107–1113. [PubMed: 16826043]
10. Ridgway JM, Armstrong WB, Guo S, et al. In vivo optical coherence tomography of the human oral cavity and oropharynx. *Arch Otolaryngol Head Neck Surg* 2006;132:1074–1081. [PubMed: 17043254]
11. Walner DL, Loewen MS, Kimura RE. Neonatal subglottic stenosis – incidence and trends. *Laryngoscope* 2001;111:48–51. [PubMed: 11192899]
12. Walner DL, Stern Y, Gerber ME, Rudolph C, Baldwin CY, Cotton RT. Gastroesophageal reflux in patients with subglottic stenosis. *Arch Otolaryngol Head Neck Surg* 1998;124:551–555. [PubMed: 9604982]
13. Tearney GJ, Jang IK, Bouma BE. Optical coherence tomography for imaging the vulnerable plaque. *J Biomed Opt* 2006;11:021002. [PubMed: 16674177]
14. Seitz U, Freund J, Jaeckle S, et al. First in vivo optical coherence tomography in the human bile duct. *Endoscopy* 2001;33:1018–1021. [PubMed: 11740643]
15. Jung W, Zhang J, Mina-Araghi R, et al. Feasibility study of normal and septic tracheal imaging using optical coherence tomography. *Lasers Surg Med* 2004;35:121–127. [PubMed: 15334615]

16. Hanna N, Saltzman D, Mukai D, et al. Two-dimensional and 3-dimensional optical coherence tomographic Imaging of the airway, lung, and pleura. *J Thorac Cardiovasc Surg* 2005;129:615–622. [PubMed: 15746746]
17. Wong B, de Boer JF, Park BH, Chen Z, Nelson JS. Optical coherence tomography of the rat cochlea. *J Biomed Opt* 2000;5:367–370. [PubMed: 11092423]
18. Wong B, Zhao Y, Yamaguchi M, Nassif N, Chen Z, De Boer JF. Imaging the internal structure of the rat cochlea using optical coherence tomography at 0.827 μm and 1.3 μm . *Otolaryngol Head Neck Surg* 2004;130:334–338. [Erratum in *Otolaryngol Head Neck Sing* 2004;130:458.]. [PubMed: 15054375]
19. Sergeev AM, Gelikonov VM, Gelikonov GV, et al. In vivo endoscopic OCT imaging of precancer and cancer states of human mucosa. *Opt Express* 1997;1:432–440. [PubMed: 19377567]
20. Shakhov AV, Terentjeva AB, Kamensky VA, et al. Optical coherence tomography monitoring for laser surgery of laryngeal carcinoma. *J Surg Oncol* 2001;77:253–258. [PubMed: 11473374]

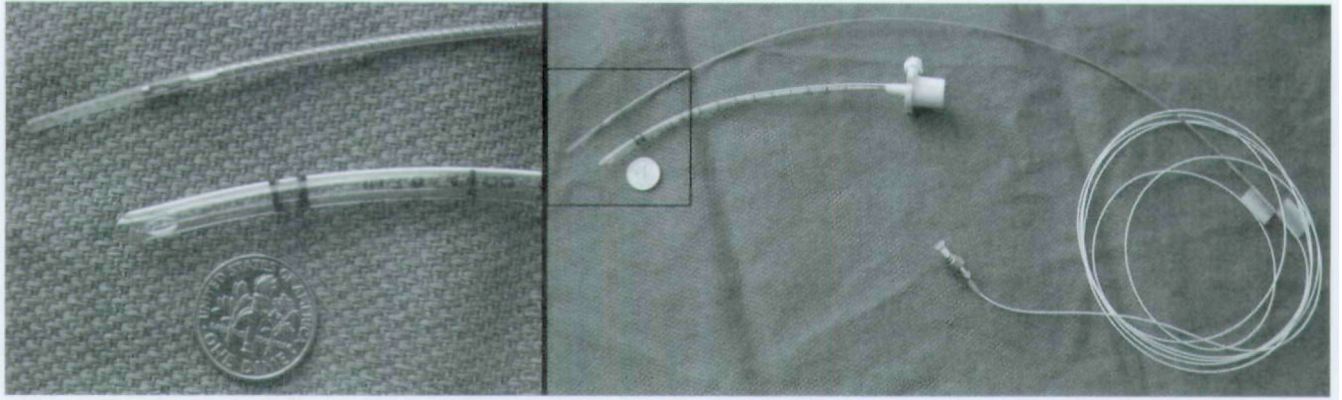


Fig 1.
Photographs of optical coherence tomography (OCT) probe for newborns.



Fig 2.
Trans-endotracheal OCT imaging with handheld probe in neonatal intensive care unit.

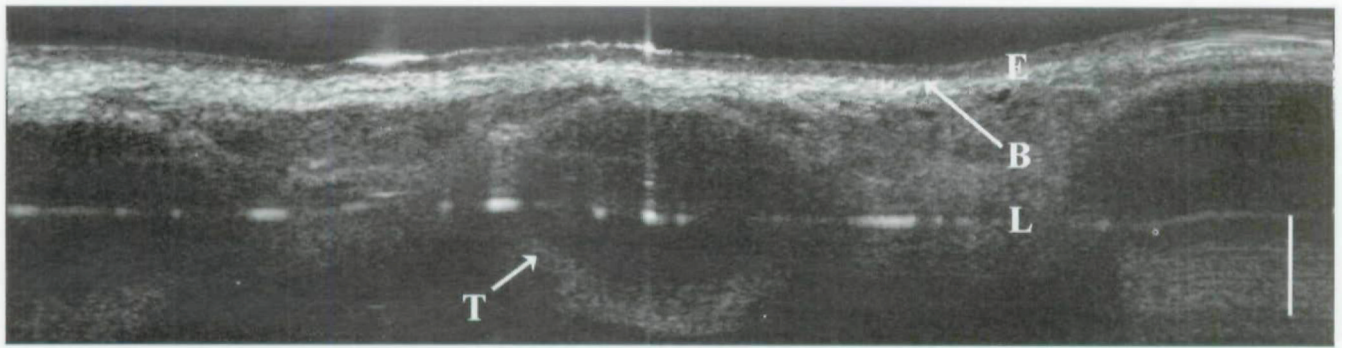


Fig 3.
OCT image of newborn trachea. E – epithelium; B – basement membrane; L – lamina propria;
T – tracheal cartilage; bar – 500 μ m.

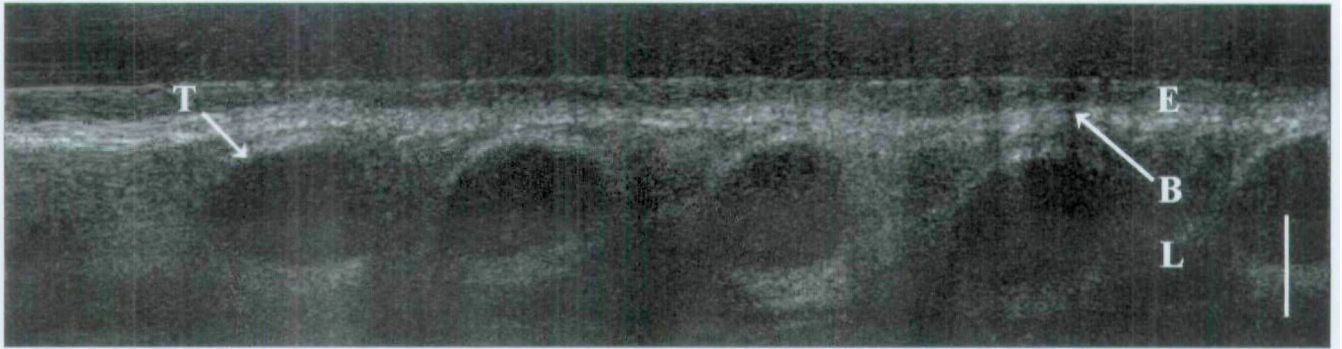


Fig 4. Trans-endotracheal OCT image of newborn trachea. E – epithelium; B – basement membrane; L – lamina propria; T – tracheal cartilage; bar – 500 μ m.

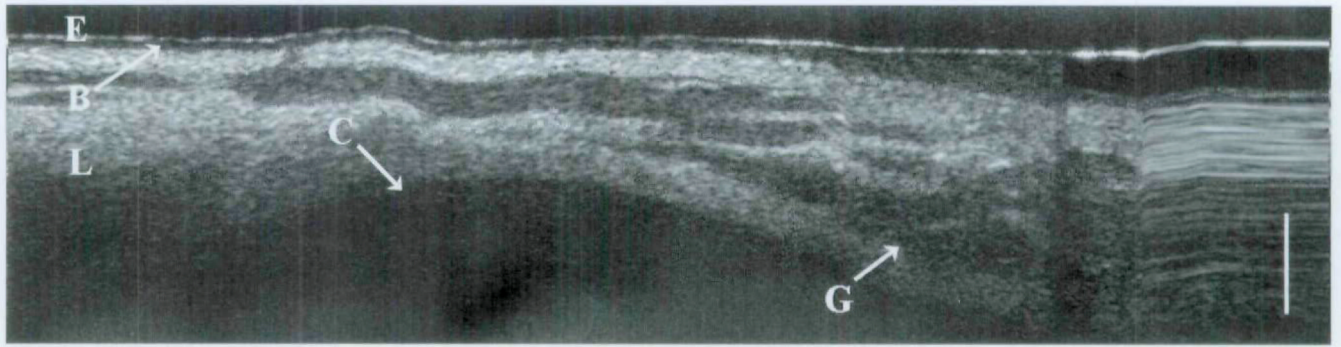


Fig 5. OCT image of newborn cricoid cartilage. E – epithelium; B – basement membrane; L – lamina propria; C – cricoid cartilage; G – glandular structures; bar – 500 μ m.

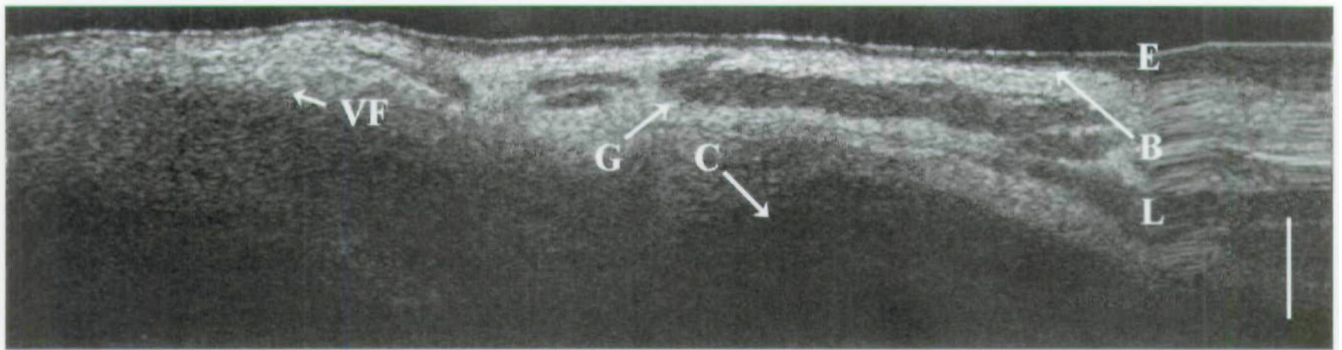


Fig 6. OCT image of newborn subglottis. E – epithelium; B – basement membrane; L – lamina propria; C – cricoid cartilage; G – glandular structures; VF – vocal fold; bar – 500 μ m.

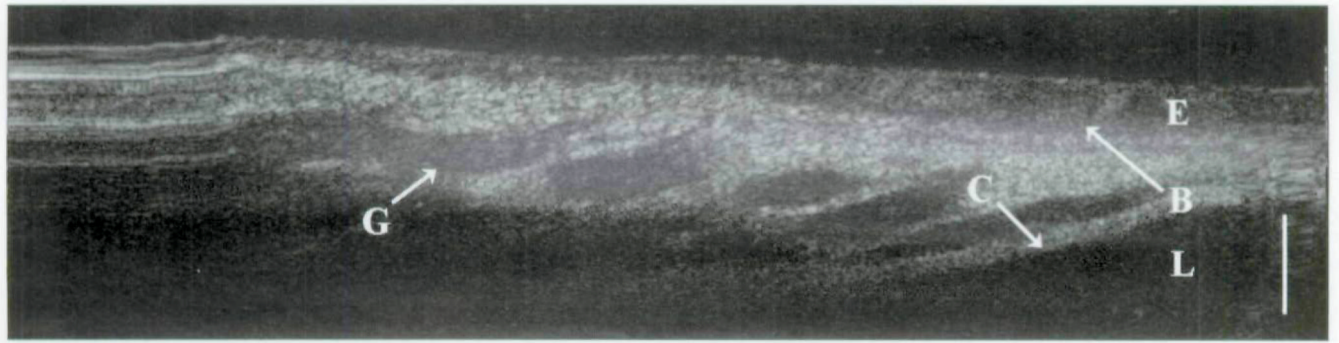


Fig 7. Trans-endotracheal OCT image of newborn subglottis. E – epithelium; B – basement membrane; L – lamina propria; C – cricoid cartilage; G – glandular structures; bar – 500 μ m.

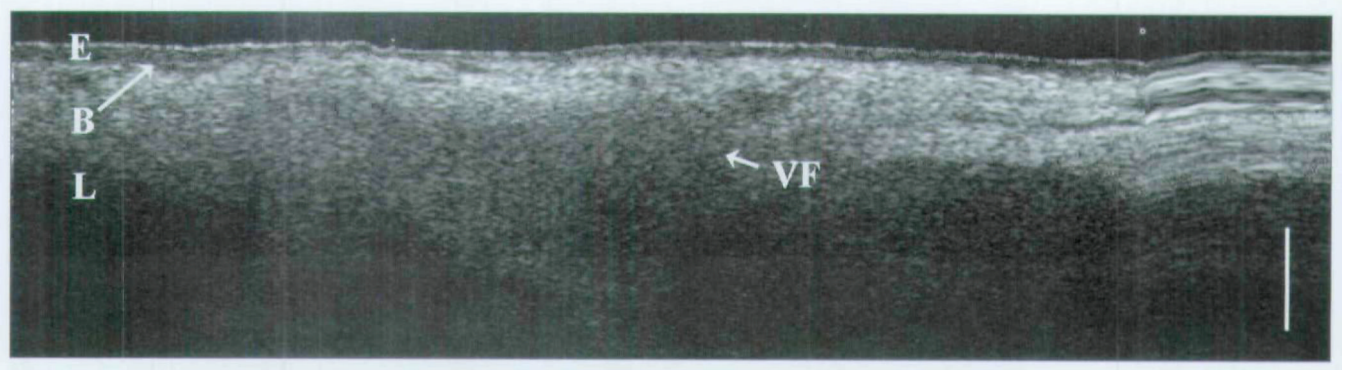


Fig 8.
OCT image of newborn glottis. E – epithelium; B – basement membrane; L – lamina propria;
VF – vocal fold; bar – 500 μ m.

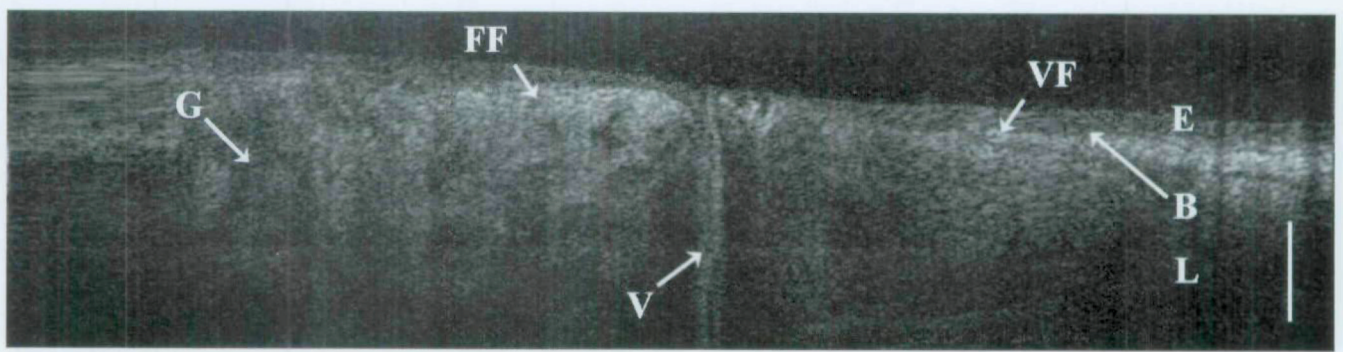


Fig 9. Trans-endotracheal OCT image of newborn false vocal fold (FF) and true vocal fold (VF). E – epithelium; B – basement membrane; L – lamina propria; G – glandular structures; V – ventricle; bar – 500 μ m.

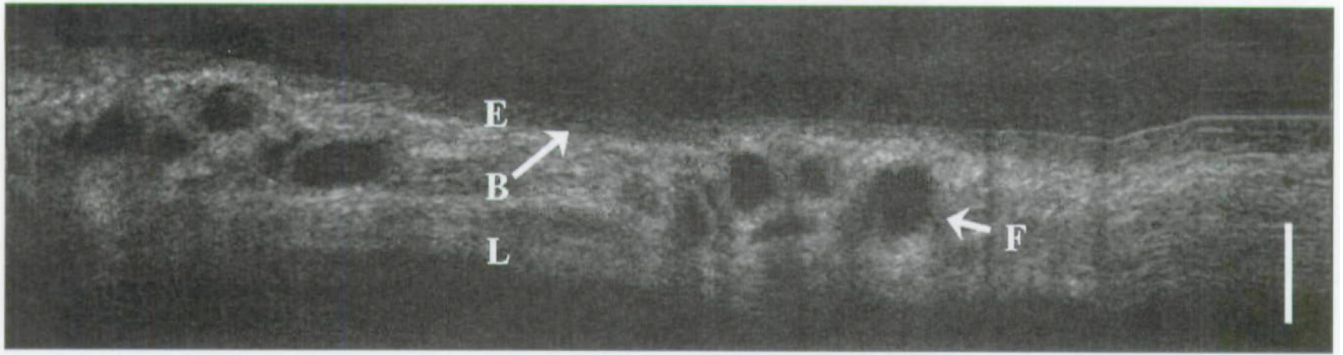


Fig 10. Trans-endotracheal OCT image of subglottis in prolonged intubation. E – epithelium; B – basement membrane; L – lamina propria; F – fluid; bar – 500 μ m.

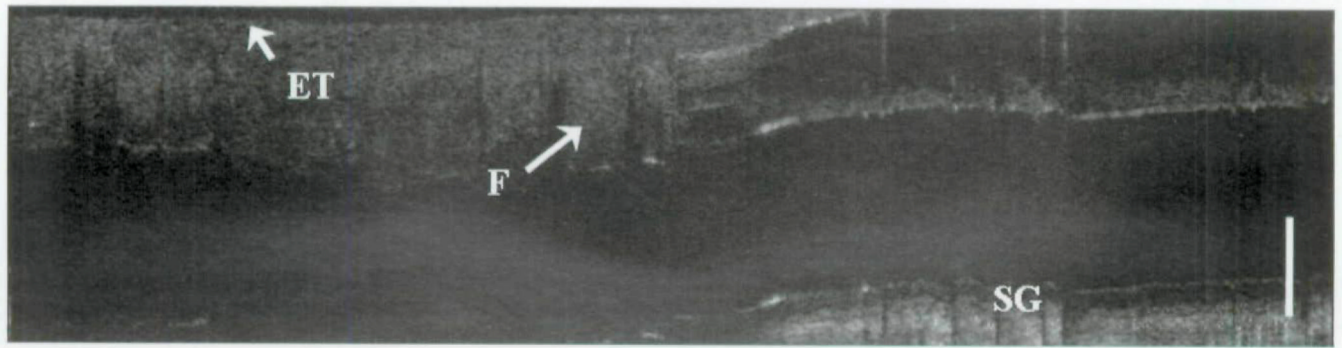


Fig 11.
Trans-endotracheal OCT image of fluid lining outside of endotracheal tube. ET – outer rim (black) of endotracheal tube; F – fluid; SG – subglottic tissue; bar – 500 μm .

BASIC NEWBORN PARAMETERS AT TIME OF OPTICAL COHERENCE TOMOGRAPHY IMAGING

Patient No.	Gestational Age* (wk)	Chronological	Weight at at Time of Imaging (g)	Duration of Intubation (h)
		Age [†] at Time of Imaging (d)		
1	40	6	3,373	1.5
2	41	27	3,238	0
3	24	61	1,336	1,464
4	27	21	1,043	504
5	32	8	1,762	144
6	26	13	657	312
7	40	2	3,704	24
8	25	0.54	586	13
9	25	0.5	800	12
10	25	0.46	610	11
11	37	26	3,610	600
12	33	0.25	1,939	6
Average	31.3	13.8	1,888.2	257.6

* Time elapsed between first day of last menstrual period and day of delivery.

[†] Time elapsed since birth.